Time-Resolved Fluorescence Investigation of the Human Immunodeficiency Virus Type 1 Nucleocapsid Protein: Influence of the Binding of Nucleic Acids

Elisa Bombarda,* Abdessamad Ababou,* Constance Vuilleumier,* Dominique Gérard,* Bernard P. Roques,# Etienne Piémont,* and Yves Mély*

*Laboratoire de Biophysique, URA 491 du CNRS, Faculté de Pharmacie, Université Louis Pasteur, B.P. 24, F-67401 Illkirch Cedex, and #Unité de Pharmacochimie Moléculaire, U 266 INSERM, URA D1500 CNRS, Faculté de Pharmacie, F-75270 Paris Cedex 06, France

ABSTRACT Depending on the HIV-1 isolate, MN or BH10, the nucleocapsid protein, NCp7, corresponds to a 55- or 71-amino acid length product, respectively. The MN NCp7 contains a single Trp residue at position 37 in the distal zinc finger motif, and the BH10 NCp7 contains an additional Trp, at position 61 in the C-terminal chain. The time-resolved intensity decay parameters of the zinc-saturated BH10 NCp7 were determined and compared to those of single-Trp-containing derivatives. The fluorescence decay of BH10 NCp7 could be clearly represented as a linear combination (with respect to both lifetimes and fractional intensities) of the individual emitting Trp residues. This suggested the absence of interactions between the two Trp residues, a feature that was confirmed by molecular modeling and fluorescence energy transfer studies. In the presence of $tRNA^{Phe}$, taken as a RNA model, the same conclusions hold true despite the large fluorescence decrease induced by the binding of $tRNA^{Phe}$. Indeed, the fluorescence of Trp^{37} appears almost fully quenched, in keeping with a stacking of this residue with the bases of $tRNA^{Phe}$. Despite the multiple binding sites in $tRNA^{Phe}$, the large prevalence of ultrashort lifetimes, associated with the stacking of Trp^{37}, suggests that this stacking constitutes a major feature in the binding process of NCp7 to nucleic acids. In contrast, Trp^{61} only stacked to a small extent with $tRNA^{Phe}$. The behavior of this residue in the $tRNA^{Phe}$-NCp7 complexes appeared to be rather heterogeneous, suggesting that it does not constitute a major determinant in the binding process. Finally, our data suggested that the binding of NCp7 proteins from the two HIV-1 strains to nonspecific nucleic acid sequences was largely similar.

INTRODUCTION

The nucleocapsid protein (NCp7) of human immunodeficiency virus type 1 (HIV-1) constitutes the ultimate cleavage product of the *gag*-encoded Pr55 polyprotein. Depending on the HIV-1 isolate, MN or BH10, NCp7 corresponds to a 55- or 71-amino acid length product, respectively (Sheng and Erickson-Viitanen, 1994). The main difference between the two products is the presence in the latter case of a longer C-terminal chain (Fig. 1). NCp7 proteins are highly basic and are characterized by two Cys-X_2-Cys-X_4-His-X_4-Cys retroviral-type zinc fingers, also referred to as CCHC motifs (Berg, 1986), which have been shown to strongly bind zinc both in vitro (Mély et al., 1996) and in mature virus preparations (Bess et al., 1992; Summers et al., 1992). Besides the two CCHC motifs, NCp7 proteins are characterized by three additional regions: the N- and C-terminal chains and a linker region between the two finger motifs. The structure of (1–72)NCp7 has been determined from ^1H NMR studies (Morellet et al., 1994) and shows that the two finger motifs are higly folded and constrained, whereas the two lateral chains are almost structureless. The linker region is partly folded and brings the CCHC motifs close together (Morellet et al., 1992; Mély et al., 1994). NCp7 plays an important role in several steps of the viral cycle, notably in the encapsidation (Berkowitz et al., 1993; Clever et al., 1995), the reverse transcription (Darlix et al., 1990; Barat et al., 1989; Lapadat-Topolsky et al., 1993), and the maturation steps. Almost all of these activities are linked to either specific (Berkowitz et al., 1993; Clever et al., 1995) or nonspecific (Darlix et al., 1990; Tsuchihashi and Brown, 1994; Mély et al., 1995) binding with target nucleic acids. The various domains of NCp7 are thought to exert distinctive properties because the finger motifs are critical to activities linked to specific binding processes (Dorfman et al., 1993; Dannull et al., 1994; Berkowitz and Goff, 1994) but are dispensable in nonspecific binding processes (de Rocquigny et al., 1992; Tanchou et al., 1995), whereas the lateral N- and C-terminal chains are essential to activities linked to nonspecific binding (Berkowitz and Goff, 1994; de Rocquigny et al., 1992; Tanchou et al., 1995). Accordingly, to get further information on how NCp7 exerts its functions, it is necessary to further characterize the NCp7-nucleic acid interaction.

Fluorescence spectroscopy of Trp residues, which constitute suitable intrinsic probes, has been proved to be a powerful technique for investigating the interaction of proteins with various ligands and, notably, nucleic acids (for a review, see Eftink, 1997). This is largely due to the fact that the fluorescence of Trp is exquisitely sensitive to even minor changes in the physicochemical environment of these residues. Consequently, the analysis of the fluorescence data and especially the time-resolved fluorescence parameters could afford very precise structural and dynamic information on the Trp residue and its nearby environment.

Received for publication 15 July 1998 and in final form 9 December 1998.

Address reprint requests to Dr. Y. Mély, Laboratoire de Biophysique, URA 491 du CNRS, Faculté de Pharmacie, Université Louis Pasteur, B.P. 24, 67401 Illkirch Cedex. Tel.: 33-388676928; Fax: 33-388674011; E-mail: mely@pharma.u-strasbg.fr.

0006-3495/99/03/1561/10 $2.00

FIGURE 1 Amino acid sequences of NCp7 derivatives. In the Aca^{61}(13–64)peptide, the mutated residue Z corresponds to an acridinylalanine residue. In $(1–72)_{dd}$NCp7, each CCHC motif was deleted and replaced with two Gly residues.

However, the use of fluorescence is limited in the case of multi-Trp-containing proteins because the fluorescence signal cannot be resolved into the constituting individual emitters. Accordingly, only global information is available in this case. Site-specific mutation of Trp residues into nonfluorescent residues is an obvious approach to overcoming this limitation. However, this approach may give rise to biased results if the Trp residue is critical for the protein structure or is directly involved in the investigated binding process. Consequently, efforts must be made to carefully resolve the fluorescence decay of the native protein by using the fluorescence decay of the mutants. Attempts of this kind have been made in a few cases. In the simplest ones, the fluorescence decay of the multi-Trp protein is a linear combination of the individual emitters (Fetler et al., 1992; Meagher et al., 1998; Vos et al., 1995). However, in other proteins, the Trp-Trp energy transfer (Harris and Hudson, 1990; Willaert et al., 1992; Vos et al., 1995) or structural modifications in mutants (Royer, 1992) preclude the linear combination.

In the present study, the time-resolved fluorescence parameters of the zinc-saturated (1–72)NCp7 have been investigated in the presence and the absence of $tRNA^{Phe}$, taken as an RNA model. (1–72)NCp7 is characterized by two Trp residues, one in position 37, which is located in the folded distal CCHC motif, and one in position 61, which is located in the highly flexible C-terminal chain (Fig. 1). As the two Trp residues are located in two different regions of the protein, which are thought to interact differently with the nucleic acid targets, two mutants have been synthesized to investigate the fluorescence of the individual emitters and the independence of the two regions. The first one, (1–55)NCp7, contains the Trp^{37} residue but lacks a large part of the C-terminal chain and corresponds to the protein from the MN isolate. The second one is the fingerless $(1–72)_{dd}$NCp7, where the two CCHC motifs have been replaced by two Gly residues. This peptide contains the Trp^{61} residue and was shown to be almost as active as the native protein in activities linked to nonspecific binding to nucleic acids (de Rocquigny et al., 1992; Tanchou et al., 1995). Finally, as the independence of the Trp residues in the native protein is a critical feature in the resolution of the fluorescence decay, an Aca^{61}(13–64)NCp7 derivative (where the Trp^{61} residue was replaced by an acridinylalanine residue) was synthesized to directly check the existence of an energy transfer between the residues in positions 37 and 61.

MATERIALS AND METHODS

(1–72)NCp7 and related peptides were synthetized on solid phase (de Rocquigny et al., 1991) and saturated with an excess of Zn, with the exception of the fingerless $(1–72)_{dd}$NCp7. The buffer was 50 mM HEPES/100 mM NaCl (pH 7.5). Polyethylene glycol 20000 was added at 0.04% to minimize the protein adsorption on the quartz cells (Karpel et al., 1987; Vuilleumier et al., 1997).

Absorption spectra were recorded on a Cary 4 spectrophotometer. Fluorescence measurements were performed at 20°C on a SLM 48000 spectrofluorimeter, with a 2-nm bandwith in excitation and an 8-nm bandwith in emission. The excitation wavelength was set at 295 nm to excite selectively the Trp residue in the peptides and at 360 nm to excite the acridinylalanine residue in the Aca^{61}(13–64)NCp7 derivative. Quantum yields were determined by taking L-Trp in water ($\phi = 0.14$) as a reference (Eisinger and Navon, 1969).

The binding of $tRNA^{Phe}$ to NCp7 derivatives was monitored by following the quenching, Q_{obs}, of the peptide fluorescence upon the addition of small aliquots of $tRNA^{Phe}$. Q_{obs} was calculated using $Q_{obs} = (I_0 - I)/I_0$, where I_0 and I correspond, respectively, to the peptide fluorescence intensities in the absence and in the presence of a given concentration of $tRNA^{Phe}$. Using the Q_{obs} values and the equations of McGhee and von Hippel (1974), we recovered the binding site size, n, the observed binding constant, K_{obs}, and the maximum extent of fluorescence quenching, Q_{max}, as previously described (Mély et al., 1995).

The time-resolved fluorescence measurements were carried out with the single-photon counting time-correlated technique, using a pulse-picked frequency-tripled Ti-sapphire laser (Tsunami; Spectra-Physics) pumped by a continuous wave argon laser. The sample was excited with 2-ps pulses with a 4-MHz repetition rate. The excitation wavelength was set at 295 nm. The emission wavelength was set at 350 nm and detected after the crossing of a polarizer oriented at magic angle (54.7°), to eliminate any polarization bias due to molecular rotation. The instrumental response function, recorded with a polished aluminium reflector, has a full width at half-maximum of ~40 ps. The decays were collected at a time resolution of 25.5 ps/channel and acquired in 2048 channels. The total number of counts for a single decay was fixed at 500,000.

Data analysis of the fluorescence intensity decays was performed by the maximum entropy method (MEM) with Pulse5 software (Livesey and Brochon, 1987). A lifetime domain spanning 200 values, equally spaced on a logarithmic time scale between 10 ps and 10 ns, was routinely used in the analysis.

The distance between the residues in positions 37 and 61 was calculated by fluorescence resonance energy transfer (FRET) measurements between the native Trp^{37} (donor) and the substituted Aca^{61} (acceptor) residues in the Aca^{61}(13–64)NCp7 derivative. The average distance R between the donor and the acceptor was computed from both the quenching of the donor and the sensitized emission of the acceptor. In the first case, the efficiency of transfer was calculated by

$$E_D = 1 - \frac{X_{DA}}{X_D} \quad (1)$$

where X_D and X_{DA} correspond to the fluorescence quantum yield (or mean lifetime) of the donor in the absence and in the presence, respectively, of the acceptor. Using the sensitized fluorescence emission of the acceptor, the transfer efficiency is calculated by

$$E_A = \frac{A_A}{A_D}\left(\frac{F_{AD}}{F_A} - 1\right) \quad (2)$$

where F_{AD} and F_A are the emission intensities in the presence and in the absence of the donor, respectively, whereas A_A and A_D are the absorbances at the donor excitation wavelength of the acceptor and the donor, respectively (Schiller, 1975). The emission intensities were corrected from screening effects at both excitation and emission wavelengths according to the method of Pigault and Gérard (1984).

The Förster critical distance R_0 was calculated according to

$$R_0 = 8.79 \times 10^{23}(n^{-4}Q_D\kappa^2 J_{AD})^{1/6}\text{Å} \quad (3)$$

where n is the refractive index of the medium (a value of 1.333 is usually taken), Q_D is the quantum yield of the donor, J_{AD} is the overlap integral calculated from the overlap between the emission spectrum of the donor and the absorbance spectrum of the acceptor (Schiller, 1975), and κ^2 is the orientational factor.

Finally, using R_0 and either E_A or E_D, the distance, R, between the acceptor and the donor is calculated using

$$R = R_0\left(\frac{1}{E} - 1\right)^{1/6} \quad (4)$$

RESULTS

Fluorescence intensity decay of NCp7 derivatives

In a previous study (Mély et al., 1996), it has been shown that both Trp^{37} and Trp^{61} are fully exposed to the solvent, a feature that is fully consistent with the (1–72)NCp7 structure (Morellet et al., 1994). The quantum yield of Trp^{37} in (1–55)NCp7 is 0.183 and is ~50% higher than that of Trp^{61} in $(1–72)_{dd}$NCp7 (Mély et al., 1996). Noticeably, the quantum yield of the native protein is intermediate and corresponds to the arithmetic average of the quantum yields of the individual Trp residues in the mutants.

The fluorescence decay parameters of (1–72)NCp7 and its derivatives are reported in Table 1. Both (1–55)NCp7 and $(1–72)_{dd}$NCp7 show a trimodal distribution. In the case of the Trp^{37}-containing (1–55)NCp7 peptide, the three lifetime peaks are well separated (Fig. 2), and the main contribution to the fluorescence decay of Trp^{37} is given by the long-lived lifetime class, which contributes ~66% of the total fluorescence intensity. In contrast, the fluorescence of Trp^{61} in $(1–72)_{dd}$NCp7 is dominated by the medium-lived lifetime class, which contributes ~51% of the total fluorescence intensity. Whereas the short-lived lifetimes were very similar in the two peptides, the medium-lived lifetimes differed by a factor of 1.3, and the long-lived ones differed by a factor of 1.42. Moreover, the distributions of the Trp^{61} lifetime peaks were rather large, and a significant overlap occurred between the medium- and long-lived lifetime peaks (Fig. 2). As expected, the $\phi/\langle\tau\rangle$ ratios of the two residues ($\sim 4.5 \times 10^7\ s^{-1}$) were fully consistent with the radiative rate of a fully solvent-exposed Trp residue (Werner and Förster, 1979).

Despite the significant differences between the lifetimes of Trp^{37} and Trp^{61}, the fluorescence decay of the native protein was also characterized by a trimodal distribution.

TABLE 1 Fluorescence decay parameters of NCp7 derivatives

	τ_i (ns)*	α_i*	f_i*	$\langle\tau\rangle$ (ns)	ϕ¶
(1–55)NCp7	6.9 (±0.3)	0.39 (±0.08)	0.66 (±0.09)	4.1 (±0.2)	0.183 (±0.003)
	3.9 (±0.3)	0.30 (±0.06)	0.28 (±0.08)		
	0.78 (±0.05)	0.31 (±0.04)	0.06 (±0.01)		
$(1–72)_{dd}$NCp7	4.8 (±0.1)	0.19 (±0.03)	0.38 (±0.05)	2.51 (±0.03)	0.121 (±0.003)
	3.01 (±0.09)	0.43 (±0.03)	0.51 (±0.05)		
	0.74 (±0.03)	0.38 (±0.01)	0.11 (±0.01)		
NCp7	6.5 (±0.1)	0.24 (±0.02)	0.50 (±0.04)	3.13 (±0.04)	0.153 (±0.003)
	3.3 (±0.1)	0.39 (±0.03)	0.41 (±0.04)		
	0.72 (±0.03)	0.36 (±0.01)	0.08 (±0.01)		
NCp7	6.32	0.28	0.54	3.29	
linear combination model#	3.41	0.37	0.38		
	0.75	0.35	0.08		
NCp7	6.3 (±0.1)	0.25 (±0.02)	0.50 (±0.03)	3.17 (±0.04)	
MEM analysis of sum-decay§	3.3 (±0.1)	0.39 (±0.02)	0.41 (±0.03)		
	0.79 (±0.07)	0.36 (±0.01)	0.09 (±0.01)		
Aca61(13–64)NCp7	4.1 (±0.1)	0.12 (±0.02)	0.37 (±0.03)	1.30 (±0.01)	
	2.17 (±0.08)	0.25 (±0.01)	0.42 (±0.03)		
	0.61 (±0.01)	0.40 (±0.01)	0.19 (±0.01)		
	0.11 (±0.01)	0.23 (±0.02)	0.020 (±0.001)		

* The barycenter value, τ_i, the relative proportion, α_i, and the fractional intensity, f_i, of each lifetime class and the mean fluorescence lifetime $\langle\tau\rangle$ are expressed as mean ± standard error of the mean for three experiments.

In the linear combination model, the values are calculated from Eqs. 5 and 6, as described in the text.

§ The reconstructed decay was obtained from the single Trp-containing derivatives and analyzed as described in the text.

¶ Values are from Mély et al. (1996).

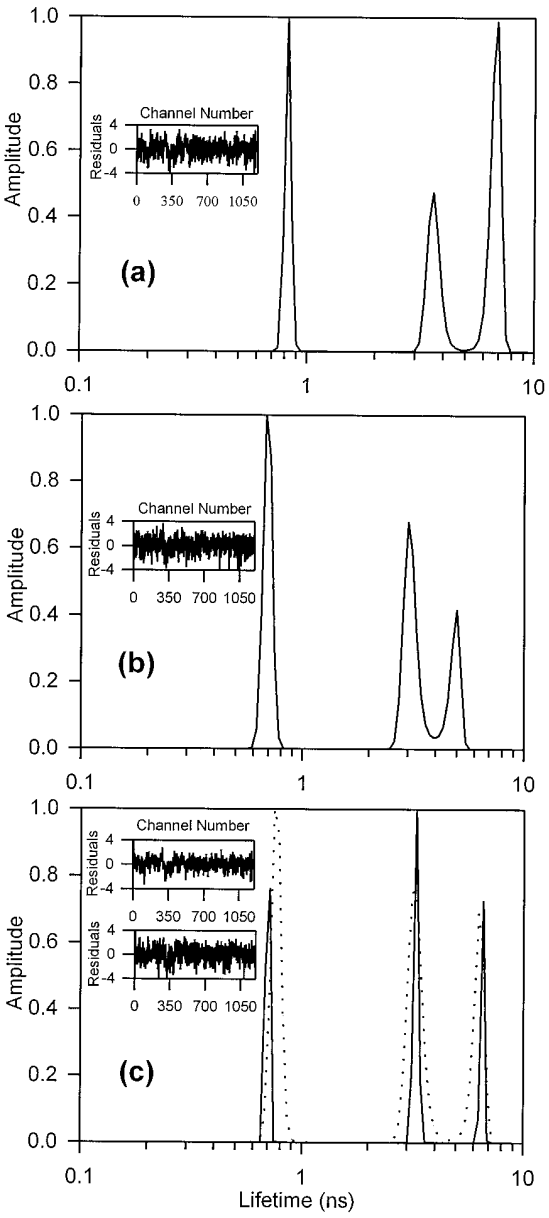

FIGURE 2 Fluorescence lifetime distributions of NCp7 derivatives. The lifetime distributions were recovered by MEM for (*a*) (1–55)NCp7, (*b*) $(1–72)_{dd}$NCp7, and (*c*) (1–72) NCp7, as described in Materials and Methods. The dotted line in *c* corresponds to the MEM analysis of the reconstructed decay obtained from the rough decay data of (1–55)NCp7 and $(1–72)_{dd}$NCp7, as described in the text. The weighted residuals for each decay are given in the insets and show only random deviation.

The short-lived lifetime class was clearly analogous to that of the two mutants, whereas the medium- and the long-lived lifetime classes showed values that are intermediate between those of the two mutants. Such a collapse has already been reported for the two Trp residues of the *lac* repressor (Royer et al., 1990) and is in line with the limitations of the time-resolved measurements and data analysis, which preclude the resolution of components that differ by less than a factor of 1.4–1.7 (Siemiarczuk et al., 1990; Vix and Lami, 1995). The point was then to determine whether the fluorescence decay of (1–72)NCp7 corresponded to the weighted average of the individual decay components. This requires that the components of the mutants be present in the wild type in the amounts dictated by their own contributions to the fluorescence of each tryptophan and the relative quantum yields of each tryptophan in the wild type. Making the reasonable assumption that the absorbances of the two solvent-exposed Trp residues are the same, the fluorescence lifetimes, τ_i^{WT}, of (1–72)NCp7 should be given by

$$\tau_i^{WT} = \frac{\phi^a f_i^a \tau_i^a + \phi^b f_i^b \tau_i^b}{\phi^a f_i^a + \phi^b f_i^b} \quad (5)$$

where *a* and *b* designate Trp^{37} and Trp^{61}, respectively, whereas ϕ, τ, and *f* are the fluorescence quantum yield, lifetime, and intensity, respectively. Similarly, the fluorescence intensities associated with each lifetime of (1–72)NCp7 should be given by

$$f_i^{WT} = \frac{\phi^a f_i^a + \phi^b f_i^b}{\phi^a + \phi^b} \quad (6)$$

The parameters calculated by Eqs. 5 and 6 are given in Table 1 and are in very good agreement with the experimental values. This is strongly in favor of the linear combination hypothesis and suggests that there is no interaction between the two Trp residues. To further check the validity of the linear combination hypothesis, we simulated the decay of (1–72)NCp7 by adding the rough decay data of the two single-Trp-containing derivatives. Of course, we took care that in the summation, the ratio between the quantum yields of the two Trp residues was respected. Moreover, so as not to introduce any bias, we ensured that there was the same total number of counts in the reconstructed decay as in the real one. Both the fluorescence lifetimes and intensities recovered by MEM analysis on the reconstructed decay are in excellent agreement with the real ones (Table 1). This reconstruction was repeated with various sets of decays and was found to be highly reproducible. This confirms that the data analysis is unable to recover the components of the two isolated Trp residues and that there is indeed a collapse between the medium-lived components of the two Trp residues and a collapse between the long-lived components of the two Trp residues. In fact, the only difference between the real and simulated data concerns the width of the lifetime distribution, which is significantly narrower in the real data (Fig. 2). From the analysis of the single-Trp-containing derivatives, the wider distribution in the simulated data may primarily arise from Trp^{61} in $(1–72)_{dd}$NCp7, and this may pinpoint minor differences of this Trp residue in $(1–72)_{dd}$NCp7 as compared to (1–72)NCp7. Taken together, our data strongly suggest that the two Trp residues behave in (1–72)NCp7 as in the single-Trp-containing derivatives and do not interact.

Independence of the two Trp residues in (1–72)NCp7

To definitively assess the independence of Trp^{37} and Trp^{61} in (1–72)NCp7, two complementary approaches were undertaken. The first one was to measure from the tertiary structure of (1–72)NCp7 (Morellet et al., 1994) the distances between the two Trp residues. The difficulty in this approach is that the Trp^{61}-containing C-terminal chain is highly flexible and may adopt different positions as compared to the CCHC fingers. Using four of the best conformers deduced by molecular modeling from ^1H NMR data, we found that the distance between the centers of the two Trp residues was between 27 and 34 Å. These distances were then used to calculate the theoretical energy transfer between the two Trp residues and its contribution to the fluorescence lifetimes. To this end, we further needed to calculate the Förster critical distance, according to Eq. 3. The overlap integral, J_{AD}, was calculated from the emission spectrum of Trp^{37} in (1–55)NCp7 and the absorption spectrum of Trp^{61} in $(1–72)_{dd}$NCp7. A value of 2/3 was taken for κ^2, a reasonable assumption with regard to the high flexibility of the Trp^{61}-containing C-terminal chain. The data are given in Table 2. Using the shortest distance from molecular modeling, we found that the energy transfer between Trp^{37} and Trp^{61} is as low as 0.01 and does not contribute significantly to the fluorescence lifetimes. The backward energy transfer ($Trp^{61} \rightarrow Trp^{37}$) is even lower and could also be neglected. However, because of the flexibility of the lateral chain, we cannot exclude the existence of conformers with a significantly shorter distance between the two Trp residues.

Accordingly, a second approach using the FRET technique was undertaken to further confirm the independence of the two Trp residues. Indeed, FRET has been shown in numerous proteins to allow a confident and direct measurement of the distance between two residues (for a review, see Eftink, 1991). However, because the two solvent-exposed Trp residues have very similar fluorescence properties and because their overlap integral is rather low, giving a short Förster distance, the Trp-Trp couple is not ideally suited to measurement of this distance. To this end, an Aca^{61}(13–64)NCp7 derivative where Trp^{61} was replaced by an acridinylalanine residue (whose absorption spectrum strongly overlaps the emission of Trp) was synthesized. The time-resolved decay of this derivative at a 350-nm emission wavelength, where the acridine moiety does not emit, showed a significant decrease in the three lifetime classes and the associated relative proportions (Table 1) of Trp^{37}. Moreover, an ultrashort lifetime (110 ps) that does not exist in the related acridine-lacking derivative appeared. Noticeably, the width of all lifetime classes was largely increased (data not shown), as compared to the related acridinylalanine-lacking derivative, and constituted a further argument for the existence of energy transfer between Trp^{37} and the acridine moiety (Eftink, 1991). Because of the multiple lifetime classes in both (1–55)NCp7 and Aca^{61}(13–64)NCp7 and in the absence of an obvious correlation in the relative proportions of the lifetime classes in the two peptides, the recovery of the energy transfer efficiency from the analysis of the lifetime classes is rather difficult. However, a mean energy transfer efficiency could be deduced from Eq. 1, if the mean lifetime values are taken. A value as high as 0.68 was obtained in these conditions. The transfer efficiency was also determined from the steady-state measurements of both the quenching of the donor and the sensitized emission of the acceptor. The transfer efficiencies, E_D and E_A, calculated in the two cases (0.76 and 0.53, respectively) were not in agreement and suggested the existence of quenching mechanisms in addition to dipolar energy transfer (Berman et al., 1980). In this case, the effective transfer efficiency, E, can be deduced by (Berman et al., 1980)

$$E = \frac{E_A}{E_A - E_D + 1} \tag{7}$$

The corrected E values for both steady-state and time-resolved data are reported in Table 2 and were in reasonable agreement. The overlap integral, $J_{AD} = 6.8 \times 10^{-15}$ M^{-1} cm^3, was then calculated from the emission spectrum of Trp^{37} in (1–55)NCp7 and the absorption spectrum of Aca^{61} in Aca^{61}(13–64)NCp7, and a value of 2/3 was taken for κ^2, a reasonable assumption with regard to the high flexibility of the Aca^{61}-containing C-terminal chain. The Förster distance, calculated using Eq. 3, was 24.8 Å. Finally, an average distance of 22–23 Å between Trp^{37} and Aca ^{61} was calculated from Eq. 4. These distances were somewhat shorter than those determined from molecular modeling. This slight discrepancy may be explained by 1) a conformational modification of the C-terminal chain induced by the substitution of Trp^{61} by the acridinylalanine residue; 2) the significant larger dimensions of the anthracene moiety of Aca as compared to the indole moiety of Trp, which may allow a closer approach to Trp^{37}; 3) a deviation of κ^2 from

TABLE 2 Calculation of the fluorescence resonance energy transfer efficiencies of the Trp^{37}-Trp^{61} pair in NCp7

	$E(Trp^{37}$-$Aca^{61})$*	$R(37–61)^{\#}$ (Å)	$J_{DA}{}^{\S}$ (M^{-1} cm^3)	R_o $(37–61)^{\P}$ (Å)	$E(Trp^{37}$-$Trp^{61})$	R_o $(61–37)^{\P}$ (Å)	$E(Trp^{61}$-$Trp^{37})^{\P}$
Molecular modeling	—	27–34			0.003–0.011		0.002–0.007
Quantum yield	0.68	22	1.25×10^{-16}	12.7	0.04	11.9	0.03
Mean lifetime	0.63	23			0.03		0.02

* The efficiency of transfer between Trp^{37} and Aca^{61} was calculated from Eq. 7 as described in the text.

$^{\#}$ R(37–61) designates the distance between the residues in position 37 and 61, calculated from molecular modeling and FRET.

§ J_{DA} is the overlap integral of the Trp^{37}-Trp^{61} pair.

¶ Critical Föster distances and related efficiencies for forward and backward energy transfer between Trp^{37} and Trp^{61}.

2/3 in either the native or the substituted derivative; or 4) the existence of conformations with shorter Trp^{37}-Trp^{61} distances that were disregarded in molecular modeling. However, the theoretical Trp^{37}-Trp^{61} forward and backward energy transfer efficiencies calculated from the FRET distances were lower than 4% (Table 2) and again could not significantly affect the fluorescence lifetimes. Indeed, by using these energy transfer efficiencies in the formulae 4–6 from Willaert et al. (1992), which were derived from the formalism of Porter (1972) for energy transfer between two identical fluorophores, it could easily be shown that the theoretical lifetimes of the two Trp residues in the wild-type species are within the standard errors of the lifetime values of these residues in the single Trp-containing mutants. Taken together, our data strongly suggested the independence of the two Trp residues.

Binding parameters of NCp7 derivatives to $tRNA^{Phe}$

To investigate the fate of the two Trp residues of (1–72)NCp7 in the NCp7-nucleic acid complex, we analyzed the behavior of (1–72)NCp7 and the two single Trp-containing derivatives: (1–55)NCp7 and $(1–72)_{dd}$NCp7 in the presence of $tRNA^{Phe}$, taken as an RNA model. As a first step, we investigated by steady-state fluorescence titration the binding parameters of these NCp7 derivatives to $tRNA^{Phe}$ (Table 3). Moreover, the electrostatic and the nonelectrostatic contributions of the binding process were determined by using salt-back reverse titrations as previously described (Mély et al., 1995).

The maximum extent of quenching, Q_{max}, of the Trp^{37} residue was very high (close to 90%) in (1–55)NCp7 (Fig. 3 and Table 3). In contrast, the quenching of Trp^{61} in $(1–72)_{dd}$NCp7 was much lower, because less than half of its fluorescence was quenched in the presence of an excess of $tRNA^{Phe}$. Moreover, the Q_{max} value of (1–72)NCp7, which contains both Trp residues, corresponded to the weighted average of the Q_{max} values of the single Trp-containing derivatives. This suggests that the two Trp residues may also behave independently in the interaction with the nucleic acid. Noticeably, the Q_{max} value and the binding parameters of (1–72)NCp7 to $tRNA^{Phe}$ obtained in the present study were slightly lower than those previously published by us (Mély et al., 1995); this may be attributed to the presence in the present study of PEG 20000 that prevented the adsorption of (1–72)NCp7 to the quartz cell walls (Vuilleumier et al., 1997). The binding constants of the various peptides were rather close because the binding constant of the most affine one, (1–72)NCp7, was only two- to threefold higher than that of the less affine one, $(1–72)_{dd}$NCp7. Noticeably, the difference in the binding constants increased to only ~10-fold when NCp7 was compared to a (12–53)NCp7 derivative that lacks both N- and C-terminal chains (data not shown). In contrast to the binding constants, significant variations were observed in the binding site sizes. Indeed, whereas the binding site size of (1–55)NCp7 was rather small but identical to that deduced by Fisher et al. (1998) from the interaction of (1–55)NCp7 with oligonucleotides, there was a significant increase in the binding site size of (1–72)NCp7 and a still larger one for that of $(1–72)_{dd}$NCp7. Whereas the binding size increase was logical for (1–72)NCp7 as compared to (1–55)NCp7 with regard to the presence of 17 additional residues, the very large binding site size of $(1–72)_{dd}$NCp7 was surprising when compared to its rather small 44-amino acid length and suggested that $(1–72)_{dd}$NCp7 may bind in a way that is different from that of the other two peptides. Finally, the salt-back titrations revealed that about five ionic interac-

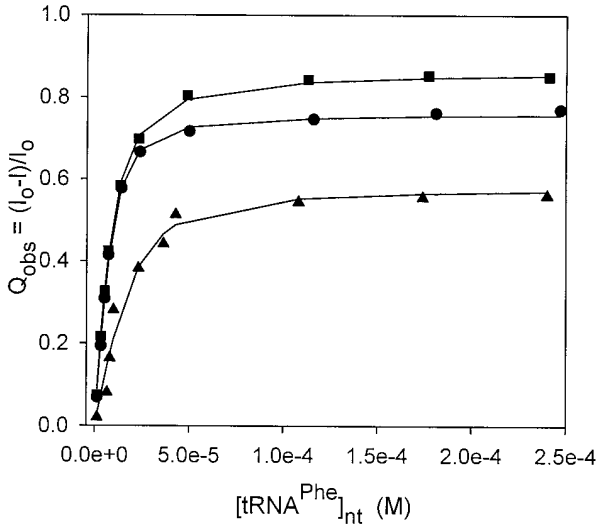

FIGURE 3 Binding isotherms of NCp7 derivatives to $tRNA^{Phe}$. The concentration of (●) (1–72)NCp7, (■) (1–55)NCp7, and (▲) $(1–72)_{dd}$NCp7 was 1 μM. Solid lines represent the best fits of the McGhee and von Hippel equation with the parameters given in Table 3.

TABLE 3 Binding parameters of NCp7 derivatives to $tRNA^{Phe}$

	Q_{max}* (%)	n*	K_{obs}* (M^{-1})	$m'^{\#}$	K_{obs} (1 M)$^{\#}$ (M^{-1})
(1–55)NCp7	87	5	3.7 (±0.9) × 10^5	4.9 (±0.2)	1.0 (±0.2) × 10^2
$(1–72)_{dd}$NCp7	46	12	2.4 (±0.2) × 10^5	4.5 (±0.2)	1.1 (±0.3) × 10^2
NCp7	73	8	5.6 (±0.4) × 10^5	4.8 (±0.5)	3.0 (±1.1) × 10^2

* The maximum extent of fluorescence quenching, Q_{max}, the binding site size, n, and the observed binding constant, K_{obs}, are calculated as described in Materials and Methods.

The number of ion pairs, m', and the intercept of the plot of log K_{obs} versus log[NaCl], K_{obs} (1 M), are calculated as means (± standard deviation) for at least three experiments.

tions were formed in the binding of both (1–72)NCp7 and (1–55)NCp7 to their binding sites on $tRNA^{Phe}$. In fact, these two proteins only differed by a threefold difference in the nonelectrostatic binding constant.

Fluorescence decay of NCp7 derivatives in the presence of nucleic acid

To further analyze the behavior of Trp^{37} and Trp^{61} in the binding process, we analyzed the time-resolved fluorescence decay of the three peptides in the presence of a 150 μM (in nucleotides) concentration of $tRNA^{Phe}$ that allows an almost full complexation of the three peptides (Fig. 3). In the case of (1–55)NCp7, the three lifetimes of Trp^{37} were slightly decreased, but the major feature was the dramatic decrease in their proportions relative to the benefit of an additional ultrashort lifetime that represented more than 60% (Table 4). In the case of $(1–72)_{dd}$NCp7, an ultrashort lifetime also appeared, but its relative proportion was less than 20%. The long-lived lifetime value of this derivative was not affected, but its relative proportion was halved. In contrast, the medium- and the short-lived lifetimes were somewhat decreased, but their relative proportions were less affected. Finally, in the wild-type protein, the situation was intermediate to that of the mutants, because the three lifetime values of (1–72)NCp7 were significantly decreased as compared to those in the absence of $tRNA^{Phe}$ (Table 1), and an ultrashort lifetime (120 ps) with a 43% relative proportion appeared. The relative proportions of both long- and medium-lived lifetime classes were decreased, but to a lesser extent than in (1–55)NCp7. Noticeably, in each peptide, the relative decreases in the fluorescence mean lifetime and quantum yield induced by the binding to $tRNA^{Phe}$ were in good agreement and suggested the absence of static quenching.

The next step was to check whether the fluorescence decay of (1–72)NCp7 complexed to $tRNA^{Phe}$ corresponded to the weighted average of the decays of the two mutants complexed to $tRNA^{Phe}$. Using the fluorescence parameters and the quantum yields of the mutants in Table 4, we calculated from Eqs. 5 and 6 the theoretical values of (1–72)NCp7 fluorescence lifetimes, τ_i^{WT}, and fluorescence intensities, f_i^{WT}. The values are reported in Table 4 and are in good agreement with the experimental values, suggesting that as in the absence of $tRNA^{Phe}$, the two Trp residues behave in (1–72)NCp7 as in the single Trp-containing derivatives and do not interact. This was confirmed by the simulated decay of (1–72)NCp7 obtained from the addition of the rough decay data of (1–55)NCp7 and $(1–72)_{dd}$NCp7. Indeed, both the fluorescence lifetimes and intensities recovered by MEM analysis (Table 4) on the reconstructed decay were in excellent agreement with the real ones. This reconstruction was repeated with various sets of decays and was found to be highly reproducible.

DISCUSSION

In the present study, the time-resolved fluorescence parameters of the two Trp-containing (1–72)NCp7 proteins were investigated and compared to those of single Trp-containing

TABLE 4 Fluorescence decay parameters of NCp7 derivatives in the presence of $tRNA^{Phe}$

	τ_i (ns)*	α_i*	f_i*	$\langle\tau\rangle$ (ns)	ϕ
(1–55)NCp7	6.1 (±0.2)	0.03 (±0.01)	0.32 (±0.07)	0.56 (±0.07)	0.024 (±0.005)
	2.2 (±0.1)	0.07 (±0.01)	0.27 (±0.06)		
	0.54 (±0.01)	0.27 (±0.01)	0.26 (±0.06)		
	0.13 (±0.01)	0.63 (±0.01)	0.15 (±0.02)		
$(1–72)_{dd}$NCp7	4.7 (±0.2)	0.09 (±0.03)	0.32 (±0.07)	1.4 (±0.2)	0.068 (±0.005)
	2.5 (±0.1)	0.25 (±0.03)	0.46 (±0.05)		
	0.58 (±0.01)	0.49 (±0.01)	0.20 (±0.04)		
	0.12 (±0.01)	0.17 (±0.01)	0.02 (±0.01)		
NCp7	4.9 (±0.2)	0.06 (±0.01)	0.32 (±0.04)	0.92 (±0.06)	0.041 (±0.005)
	2.4 (±0.1)	0.15 (±0.01)	0.39 (±0.04)		
	0.60 (±0.02)	0.36 (±0.01)	0.23 (±0.02)		
	0.12 (±0.01)	0.43 (±0.01)	0.06 (±0.01)		
NCp7	5.04	0.06	0.31	1.00	
linear combination model[#]	2.44	0.17	0.42		
	0.57	0.39	0.22		
	0.13	0.38	0.05		
NCp7	5.0 (±0.1)	0.06 (±0.01)	0.29 (±0.03)	1.0 (±0.1)	
MEM analysis of sum-decay[§]	2.4 (±0.1)	0.18 (±0.01)	0.41 (±0.03)		
	0.58 (±0.01)	0.41 (±0.02)	0.23 (±0.01)		
	0.19 (±0.01)	0.35 (±0.02)	0.07 (±0.01)		

* The barycenter value, τ_i, the relative proportion, α_i, and the fractional intensity, f_i, of each lifetime class and the mean fluorescence lifetime $\langle\tau\rangle$ are expressed as mean ± standard error of the mean for three experiments.

[#] In the linear combination model the values are calculated from Eqs. 5 and 6, as described in the text.

[§] The reconstructed decay was obtained from the single Trp-containing derivatives as described in the text.

derivatives, in both the absence and the presence of $tRNA^{Phe}$. In the absence of nucleic acid, the intensity decay components of (1–72)NCp7 could not be assigned to specific Trp residues, but are clearly a linear combination of the lifetimes associated with the individual Trp residues. This linear combination is in line with the absence of interaction between the two Trp residues, as inferred from both molecular modeling and FRET studies. Moreover, as the Trp^{37}-containing derivative, (1–55)NCp7, contains the two CCHC motifs but lacks the C-terminal chain, whereas the reverse situation appears in the Trp^{61}-containing derivative, $(1–72)_{dd}$NCp7, we further suggest that the C-terminal chain does not affect the environment of Trp^{37}, and the CCHC motifs do not affect the environment of Trp^{61}. Similarly, from the very close decay parameters of (1–55)NCp7 (this work) and (12–53)NCp7 (Mély et al., 1998), we also conclude that the N-terminal chain also does not modify the environment of Trp^{37}. The linear combination of the individual decay components in (1–72)NCp7 is in contrast to the failure of this kind of combination with the Trp residues of bacteriophage T4 lysozyme (Harris and Hudson, 1990), human epidermal growth factor (Gallay et al., 1993), Trp repressor (Royer, 1992), or barnase (Willaert et al., 1992). This failure has been attributed to either Trp-Trp resonance energy transfer or structural differences between mutants and wild-type protein. In the case of the glutamine-binding protein from *E. coli* (Axelsen et al., 1991), a linear combination was suggested, but the authors were not able to draw a conclusion about the absolute validity of this hypothesis. A similar situation prevails in the case of the *lac* repressor, where no attempts were made to determine whether the linear combination also applies to the lifetime-associated intensities (Royer et al., 1990). Finally, to our knowledge, the linear combination hypothesis has only been clearly assessed in the case of aspartate transcarbamylase (Fetler et al., 1992), human antithrombin (Meagher et al., 1998), and the two Trp-containing mutants, but not the wild-type colicinA (Vos et al., 1995). Noticeably, even in the case of aspartate transcarbamylase, some slight differences in the structural features of the mutants as compared to the wild type cannot be excluded, because the quantum yield of the wild type does not correspond to the weighted average of the quantum yields of the mutants (Fetler et al., 1992). Hence the occurrence of the linear combination hypothesis does not seem to be very common in proteins, and in this respect (1–72)NCp7 may constitute a good reference where this hypothesis clearly applies. This is mainly due to the fact that the two Trp residues are far from each other in two structurally and functionally independent domains.

Our data also illustrate the limits of the resolvability for intensity decay analysis. Indeed, there is a clear collapse of the lifetimes of the two Trp residues despite a lifetime ratio as large as 1.4 for the long-lived lifetimes. This is in line with the fact that almost all multi-Trp-containing proteins could be resolved by a bi- or trimodal analysis (Beechem and Brand, 1985), even though the individual Trp residues are also characterized by this kind of decay. More unexpectedly, the widths of the lifetime peaks were rather narrow and do not indicate that a collapse between significantly different lifetime peaks occurred. This observation is in keeping with the proposal of Swaminathan and Periasamy (1996) that the width of the lifetime peaks is sensitive to many factors (peak counts, discretization in τ space, completeness of decay, χ^2 stopping criteria, etc.) and cannot be used for quantitative interpretation of lifetime heterogeneity. In contrast to several proteins, where at least one component of the intensity decay of the wild-type protein could be unambigously attributed to one particular Trp residue (Royer et al., 1990; Fetler et al., 1992), all of the (1–72)NCp7 components correspond to a collapse of the components of the two Trp residues. Accordingly, the (1–72)NCp7 data do not allow us, upon a change in some biophysically relevant parameter, to conclude which Trp and therefore which part of the (1–72)NCp7 structure is involved in the thermodynamic or dynamic phenomenon under study. However, the comparison of (1–72)NCp7 with its mutants allows us to determine the relevance of the conclusions obtained with the mutants and the independence of (1–72)NCp7 domains in the investigated phenomenon.

This approach was applied to the interaction of (1–72)NCp7 with $tRNA^{Phe}$. Using an excess of nucleic acid, we found that the saturation of (1–55)NCp7 with $tRNA^{Phe}$ induced an almost complete quenching of the fluorescence of Trp^{37} that suggested a stacking of this residue with the bases of $tRNA^{Phe}$. A similar conclusion has been inferred with a (34–51)NCp7 peptide that corresponds to the sequence of the C-terminal finger CCHC motif (Mély et al., 1993). This strongly suggests that the presence of the N-terminal CCHC motif and the spatial proximity (Morellet et al., 1992; Mély et al., 1994) of the two CCHC motifs (and especially the proximity of Trp^{37} to Phe^{16}) do not hinder the interaction of Trp^{37} with the bases of $tRNA^{Phe}$. Moreover, the existence of a stacking of Trp^{37} with the bases of a nucleic acid has been independently assessed by phosphorescence (Lam et al., 1994; Wu et al., 1997) and NMR (Morellet et al., 1998; De Guzman et al., 1998). Despite the existence of multiple binding sites on $tRNA^{Phe}$, the binding of (1–55)NCp7 to $tRNA^{Phe}$ seems rather homogeneous with regard to the involvement of Trp^{37} in the binding process, because the relative proportion of the ultrashort lifetime associated with the stacking phenomena represented more than 60%. This suggests, in keeping with the effect of Trp^{37} mutation on virus infectivity (Dorfman et al., 1993), that the stacking interaction of Trp^{37} is critical to the binding of (1–72)NCp7 to its nucleic acid targets. Even if the stacking interaction is by far the main feature of the interaction between Trp^{37} and the nucleic acid, it is not the sole one. Indeed, a significant but limited decrease in the three major lifetimes was observed, suggesting that minor binding modes may be associated with conformational changes, without stacking, upon binding to the polynucleotide backbone (Montenay-Garestier et al., 1983).

The behavior of Trp^{61} is in clear contrast to that of Trp^{37}. Indeed, only a small fraction of the fluorescence decay of

$(1–72)_{dd}$NCp7 complexed to $tRNA^{Phe}$ appeared as an ultrashort lifetime and could be associated with a stacking of Trp^{61} with the bases. In fact, the largest part of the peptide fluorescence decrease was due to a limited decrease in the medium- and short-lived fluorescence lifetimes, which may be associated with conformational changes (without stacking) of the Trp^{61} residue, induced upon binding to the polynucleotide backbone. Furthermore, as a significant fraction of the long-lived lifetime class remained unaffected by the binding to $tRNA^{Phe}$, it may be concluded that in the peptides associated with this class, the Trp^{61} residue does not interact at all with $tRNA^{Phe}$. Moreover, a comparison of the lifetimes and the associated amplitudes in the presence of $tRNA^{Phe}$ with those in its absence does not provide any obvious interpretation. This suggests that there may be a rather large and probably sequence-dependent heterogeneity in the binding modes of Trp^{61} with $tRNA^{Phe}$. Hence we may suggest that Trp^{61} may not be critically involved in the binding process. A more precise investigation of the sequence dependence of the binding mode of both Trp residues is currently under investigation.

Using the wild-type (1–72)NCp7 protein, we found that the intensity decay in the presence of a saturating $tRNA^{Phe}$ concentration corresponds again to the weighted average of the individual emitting Trp residues in the two single Trp-containing derivatives complexed to $tRNA^{Phe}$. Hence this suggested that Trp^{37} is largely involved in stacking interactions with the nucleic acid bases of $tRNA^{Phe}$, whereas Trp^{61} seems to be only marginally involved. Moreover, because the (1–55)NCp7 derivative lacks the C-terminal chain and the $(1–72)_{dd}$NCp7 lacks the two CCHC motifs, we further infer that in (1–72)NCp7, the C-terminal chain does not hinder the interaction of Trp^{37} with $tRNA^{Phe}$ and that the CCHC motifs do not affect the interaction of Trp^{61} with $tRNA^{Phe}$. According to the structural and functional unity of the CCHC motifs on one hand and the N- and C-terminal chains on the other hand (Morellet et al., 1994; de Rocquigny et al., 1992), we may conclude that these two domains interact more or less independently with $tRNA^{Phe}$. Finally, together with the poor differences in the binding parameters of (1–72)NCp7 and (1–55)NCp7 with $tRNA^{Phe}$, the time-resolved fluorescence data suggest that the binding of NCp7 proteins from MN or BH10 strains to nucleic acids, at least to the nonspecific binding sites, was largely similar and, hence, that a large part of the C-terminal chain (residues 56–72) interacted only marginally with the nucleic acid sequence.

We are grateful to Patrice Petitjean for peptide synthesis and Nelly Morellet for the distance calculation from molecular modeling.

This work was supported by grants from the Agence Nationale de la Recherche sur le SIDA, Centre National de la Recherche Scientifique et Université Louis Pasteur.

REFERENCES

Axelsen, P. H., Z. Bajzer, F. G. Prendergast, P. F. Cottam, and C. Ho. 1991. Resolution of the fluorescence intensity decays of the two tryptophan residues in glutamine-binding protein from *Escherichia coli* using single tryptophan mutants. *Biophys. J.* 60:650–659.

Barat, C., V. Lullien, O. Schatz, G. Keith, M. T. Nugeyre, F. Grüninger-Leitch, F. Barré-Sinoussi, S. F. J. Le Grice, and J. L. Darlix. 1989. HIV-1 reverse transcriptase specifically interacts with the anticodon domain of its cognate primer tRNA. *EMBO J.* 8:3279–3285.

Beechem, J. M., and L. Brand. 1985. Time-resolved fluorescence of proteins. *Annu. Rev. Biochem.* 54:43–71.

Berg, J. M. 1986. Potential metal-binding domains in nucleic acid binding proteins. *Science.* 232:485–487.

Berkowitz, R. D., and S. P. Goff. 1994. Analysis of binding elements in the human immunodeficiency virus type 1 genomic RNA and nucleocapsid protein. *Virology.* 202:233–246.

Berkowitz, R. D., J. Luban, and S. P. Goff. 1993. Specific binding of human immunodeficiency virus type 1 *gag* polyprotein and nucleocapsid protein to viral RNAs detected by RNA mobility shift assays. *J. Virol.* 67:7190–7200.

Berman, H. A., J. Yguerabide, and P. Taylor. 1980. Fluorescence energy transfer on acetylcholinesterase: spatial relationship between peripheral site and active center. *Biochemistry.* 19:2226–2235.

Bess, J. W., Jr., P. J. Powell, H. J. Issaq, L. J. Schumack, M. K. Grimes, L. E. Henderson, and L. O. Arthur. 1992. Tightly bound zinc in human immunodeficiency virus type 1, human T-cell leukemia virus type I, and other retroviruses. *J. Virol.* 66:840–847.

Clever, J., C. Sassetti, and T. G. Parslow. 1995. RNA secondary structure and binding sites for *gag* gene products in the 5′ packaging signal of human immunodeficiency virus type 1. *J. Virol.* 69:2101–2109.

Dannull, J., A. Surovoy, G. Jung, and K. Moelling. 1994. Specific binding of the HIV-1 nucleocapsid protein to psi RNA in vitro requires N-terminal zinc finger and flanking basic amino acid residues. *EMBO J.* 13:1525–1533.

Darlix, J. L., C. Gabus, M. T. Nugeyre, F. Clavel, and F. Barré-Sinoussi. 1990. *Cis* elements and *trans*-acting factors involved in the RNA dimerization of the human immunodeficiency virus HIV-1. *J. Mol. Biol.* 216:689–699.

De Guzman, R. N., Z. R. Wu, C. C. Stalling, L. Pappalardo, P. N. Borer, and M. F. Summers. 1998. Structure of the HIV-1 nucleocapsid protein bound to the SL3 89-RNA recognition element. *Science.* 279:384–388.

de Rocquigny, H., D. Ficheux, C. Gabus, M. C. Fournié-Zaluski, J. L. Darlix, and B. P. Roques. 1991. First large scale chemical synthesis of the 72 amino acids HIV-1 nucleocapsid protein NCp7 in an active form. *Biochem. Biophys. Res. Commun.* 180:1010–1018.

de Rocquigny, H., C. Gabus, M. C. Fournié-Zaluski, B. P. Roques, and J. L. Darlix. 1992. Viral RNA annealing activities of human immunodeficiency virus type 1 nucleocapsid protein require only peptide domains outside the zinc fingers. *Proc. Natl. Acad. Sci. USA.* 89: 6472–6476.

Dorfman, T., J. Luban, S. P. Goff, W. A. Haseltine, and H. G. Göttlinger. 1993. Mapping of functionally important residues of a cysteine-histidine box in the human immunodeficiency virus type 1 nucleocapsid protein. *J. Virol.* 67:6159–6169.

Eftink, M. R. 1991. Fluorescence quenching: theory and applications. *In* Topics in Fluorescence Spectroscopy, Vol. 2, Principles. J. R. Lakowicz, editor. Plenum Press, New York. 53–120.

Eftink, M. R. 1997. Fluorescence methods for studying equilibrium macromolecule-ligand interactions. *Methods Enzymol.* 278:221–257.

Eisinger, J., and G. Navon. 1969. Fluorescence quenching and isotope effect of tryptophan. *J. Chem. Phys.* 50:2069–2077.

Fetler, L., P. Tauc, G. Hervé, M. M. Ladjimi, and J. C. Brochon. 1992. The tryptophan residues of aspartate transcarbamylase: site-directed mutagenesis and time-resolved fluorescence spectroscopy. *Biochemistry.* 31:12504–12513.

Fisher, R. J., A. Rein, M. Fivash, M. A. Urbaneja, J. R. Casas-Finet, M. Medaglia, and L. E. Henderson. 1998. Sequence-specific binding of human immunodeficiency virus type 1 nucleocapsid protein to short oligonucleotides. 72:1902–1909.

Gallay, J., M. Vincent, I. M. Li de la Sierra, J. Alvarez, R. Ubieta, J. Madrazo, and G. Padron. 1993. Protein flexibility and aggregation state of human epidermal growth factor. A time-resolved fluorescence study of the native protein and engineered single-tryptophan mutants. *Eur. J. Biochem.* 211:213–219.

Harris, D. L., and B. S. Hudson. 1990. Photophysics of tryptophan in bacteriophage T4 lysozymes. *Biochemistry.* 29:5276–5285.

Karpel, R. L., L. E. Henderson, and S. Oroszland. 1987. Interactions of retroviral structural proteins with single stranded nucleic acids. *J. Biol. Chem.* 262:4961–4967.

Lam, W. C., A. H. Maki, J. R. Casas-Finet, J. W. Erickson, B. P. Kane, R. C. Sowder II, and L. E. Henderson. 1994. Phosphorescence and optically detected magnetic resonance investigation of the binding of the nucleocapsid protein of the human immunodeficiency virus type 1 and related peptides to RNA. *Biochemistry.* 33:10693–10700.

Lapadat-Topolsky, M., H. De Rocquigny, D. Van Gent, B. Roques, R. Plasterk, and J. L. Darlix. 1993. Interaction between HIV-1 nucleocapsid protein and viral DNA may have important functions in the viral life cycle. *Nucleic Acids Res.* 21:831–839.

Livesey, A. K., and J. C. Brochon. 1987. Analyzing the distribution of decay constants in pulse-fluorimetry using the maximum entropy method. *Biophys. J.* 52:693–706.

McGhee, J. D., and P. H. von Hippel. 1974. Theoretical aspects of DNA-protein interactions: co-operative and non-co-operative binding of large ligands to a one-dimensional homogeneous lattice. *J. Mol. Biol.* 86: 469–489.

Meagher, J. L., J. M. Beechem, S. T. Olson, and P. G. W. Gettins. 1998. Deconvolution of the fluorescence emission spectrum of human antithrombin and identification of the tryptophan residues that are responsive to heparin binding. *J. Biol. Chem.* 273:23283–23289.

Mély, Y., E. Bombarda, C. Vuilleumier, H. de Rocquigny, B. P. Roques, and D. Gérard. 1998. Involvement of the aromatic aminoacid (Phe^{16} and Trp^{37}) of the HIV-1 nucleocapsid protein in the binding to the homologous $tRNA^{Lys,3}$ and the heterologous $tRNA^{Phe}$: a fluorescence spectroscopy investigation. *In* Fluorescence Microscopy and Fluorescent Probes, Vol. 2. J. Slavik, editor. Plenum Publishing Company, New York. 192–196.

Mély, Y., H. de Rocquigny, M. Sorinas-Jimeno, G. Keith, B. P. Roques, R. Marquet, and D. Gérard. 1995. Binding of the HIV-1 nucleocapsid protein to the primer $tRNA_3^{Lys}$, in vitro, is essentially nonspecific. *J. Biol. Chem.* 270:1650–1656.

Mély, Y., N. Jullian, N. Morellet, H. de Rocquigny, C. Z. Dong, E. Piémont, B. P. Roques, and D. Gérard. 1994. Spatial proximity of the HIV-1 nucleocapsid protein zinc fingers investigated by time-resolved fluorescence and fluorescence resonance energy tranfer. *Biochemistry.* 33:12085–12091.

Mély, Y., N. Morellet, H. de Rocquigny, B. P. Roques, and D. Gérard. 1996. Zinc binding to the HIV-1 nucleocapsid protein: a thermodynamic investigation by fluorescence spectroscopy. *Biochemistry.* 35: 5175–5182.

Mély, Y., E. Piémont, M. Sorinas-Jimeno, H. de Rocquigny, N. Jullian, N. Morellet, B. P. Roques, and D. Gérard. 1993. Structural and dynamic characterization of the aromatic amino acids of the human immunodeficiency virus type 1 nucleocapsid protein zinc fingers and their involvement in heterologous $tRNA^{Phe}$ binding: a steady-state and time-resolved fluorescence study. *Biophys. J.* 65:1513–1522.

Montenay-Garestier, T., F. Toulmé, J. Fidy, J. J. Toulmé, T. Le Doan, and C. Hélène. 1983. Structure and dynamics of peptide-nucleic acid complexes. *In* Structure, Dynamics and Interactions and Evolution of Biological Macromolecules. C. Hélène, editor. D. Reidel Publishing Company, Dordrecht, the Netherlands. 113–128.

Morellet, N., H. Déméné, V. Teilleux, T. Huynh-Dinh, H. de Rocquigny, M. C. Fournié-Zaluski, and B. P. Roques. 1998. Structure of the complex between the HIV-1 nucleocapsid protein NCp7 and the single-stranded pentanucleotide d(ACGCC). *J. Mol. Biol.* 283:419–434.

Morellet, N., H. de Rocquigny, Y. Mély, N. Jullian, H. Déméné, M. Ottmann, D. Gérard, J. L. Darlix, M. C. Fournié-Zaluski, and B. P. Roques. 1994. Conformational behaviour of the active and inactive forms of the nucleocapsid NCp7 of HIV-1 studied by ^{1}H NMR. *J. Mol. Biol.* 235:287–301.

Morellet, N., N. Jullian, H. de Rocquigny, B. Maigret, J. L. Darlix, and B. P. Roques. 1992. Determination of the structure of the nucleocapsid protein NCp7 from human immunodeficiency virus type 1 by ^{1}H NMR. *EMBO J.* 11:3059–3065.

Pigault, C., and D. Gérard. 1984. Influence of the location of tryptophanyl residues in proteins on their photosensitivity. *Photochem. Photobiol.* 40:291–296.

Porter, G. B. 1972. Reversible energy transfer. *Theor. Chim. Acta.* 24: 265–270.

Royer, C. 1992. Investigation of the structural determinants of the intrinsic fluorescence emission of the *trp* repressor using single tryptophan mutants. *Biophys. J.* 63:741–750.

Royer, C. A., J. A. Gardner, J. M. Beechem, J. C. Brochon, and K. S. Matthews. 1990. Resolution of the fluorescence decay of the two trptophan residues of *lac* repressor using single tryptophan mutants. *Biophys. J.* 58:363–378.

Schiller, P. W. 1975. The measurement of intramolecular distances by energy transfer. *In* Biochemical Fluorescence: Concepts. R. F. Chen and H. Edelhoch, editors. Marcel Dekker, New York. 285–303.

Sheng, N., and S. Erickson-Viitanen. 1994. Cleavage of p15 protein in vitro by human immunodeficiency virus type 1 protease is RNA dependent. *J. Virol.* 68:6207–6214.

Siemiarczuk, A., B. D. Wagner, and W. R. Ware. 1990. Comparison of the maximum entropy and exponential series methods for the recovery of distributions of lifetimes from fluorescence lifetime data. *J. Phys. Chem.* 94:1661–1666.

Summers, M. F., L. E. Henderson, M. R. Chance, J. W. Bess Jr., T. L. South, P R. Blake, I. Sagi, G. Perez-Alvarado, R. C. Sowder III, D. R. Hare, and L. O. Arthur. 1992. Nucleocapsid zinc fingers detected in retroviruses: EXAFS studies of intact viruses and the solution-state structure of the nucleocapsid protein from HIV-1. *Protein Sci.* 1:563–574.

Swaminathan, R., and N. Periasamy. 1996. Analysis of fluorescence decay by the maximum entropy method: influence of noise and analysis parameters on the width of the distribution of lifetimes. *Proc. Indian Acad. Sci.* 108:39–49.

Tanchou, V., C. Gabus, V. Rogemond, and J. L. Darlix. 1995. Formation of stable and functional HIV-1 nucleoprotein complexes in vitro. *J. Mol. Biol.* 252:563–571.

Tsuchihashi, Z., and P. O. Brown. 1994. DNA strand exchange and selective DNA annealing promoted by the human immunodeficiency virus type 1 nucleocapsid protein. *J. Virol.* 68:5863–5870.

Vix, A., and H. Lami. 1995. Protein fluorescence decay: discrete components or distribution of lifetimes? Really no way out of the dilemma? *Biophys. J.* 68:1145–1151.

Vos, R., Y. Engelborghs, J. Izard, and D. Baty. 1995. Fluorescence study of the three tryptophan residues of the pore-forming domain of colicin A using multifrequency phase fluorometry. *Biochemistry.* 34:1734–1743.

Vuilleumier, C., C. Maechling-Strasser, D. Gérard, and Y. Mély. 1997. Evidence and prevention of HIV-1 nucleocapsid protein adsorption onto fluorescence quartz cells. *Anal. Biochem.* 244:183–185.

Werner, T. C., and L. S. Förster. 1979. The fluorescence of tryptophanyl peptides. *Photochem. Photobiol.* 29:905–914.

Willaert, K, R. Loewenthal, J. Sancho, M. Froeyen, A. Fersht, and Y. Engelborghs. 1992. Determination of the excited-state lifetimes of the tryptophan residues in barnase, via multifrequency phase fluorometry of tryptophan mutants. *Biochemistry.* 31:711–716.

Wu, J. Q., A. Ozarowski, A. H. Maki, M. A. Urbaneja, L. E. Henderson, and J. R. Casas-Finet. 1997. Binding of the nucleocapsid protein of type 1 human immunodeficiency virus to nucleic acids studied using phosphorescence and optically detected magnetic resonance. *Biochemistry.* 36:12506–12518.